Rapid Communications

Ratchet effect in the quantum kicked rotor and its destruction by dynamical localization

Clément Hainaut,[1] Adam Rançon,[1] Jean-François Clément,[1] Jean Claude Garreau,[1] Pascal Szriftgiser,[1] Radu Chicireanu,[1] and Dominique Delande[2]

[1]*Université de Lille, CNRS, UMR 8523 – PhLAM – Laboratoire de Physique des Lasers Atomes et Molécules, F-59000 Lille, France*

[2]*Laboratoire Kastler Brossel, UPMC-Sorbonne Universités, CNRS, ENS-PSL Research University, Collège de France, 4 Place Jussieu, F-75005 Paris, France*

(Received 8 January 2018; published 7 June 2018)

We study experimentally a quantum kicked rotor with broken parity symmetry, supporting a ratchet effect due to the presence of a classical accelerator mode. We show that the short-time dynamics is very well described by the classical dynamics, characterized by a strongly asymmetric momentum distribution with directed motion on one side, and an anomalous diffusion on the other. At longer times, quantum effects lead to dynamical localization, causing an asymptotic resymmetrization of the wave function.

DOI: 10.1103/PhysRevA.97.061601

Quantum transport phenomena play a central role in many areas in physics, such as coherently controlled photocurrent in semiconductors [1] or atoms in optical lattices [2]. Nonlinearity can lead to interesting effects even for really simple models, with numerous applications, such as dynamics of Josephson junctions [3] and electronic transport through superlattices [4], to cite a few. Symmetries in the system are of fundamental importance, as their presence or absence can enhance or destroy (quantum) interferences, and can therefore strongly affect transport properties. In particular, in systems with broken parity symmetry, one can observe directed transport [5]. The breaking of time-reversal symmetry can also lead to directed transport [6], an example being the ratchet effect, that is, the existence of directed transport without a bias field in periodic systems.

The study of the ratchet effect was stimulated by the research on Brownian molecular motors, e.g., in biological systems, and was investigated in different simple noisy models [7]. In its original formulation, this effect is of a stochastic nature, due to an external (for instance, thermal) noise. A possible variant are the so-called Hamiltonian chaotic ratchets [8–10], where the extrinsic noise is replaced by deterministic chaos, possibly in the presence of dissipation [6,11–15]. These ratchets require mixed phase spaces displaying regular regions embedded in a chaotic sea [9]. However, it can be shown that in a Hamiltonian chaotic ratchet the current averaged on the whole phase space is always zero for unbiased potentials. The accelerated islands in phase space contribute to directed transport, but this effect is globally compensated by the motion of the remaining part of the phase space, the chaotic sea [8,9].

The kicked rotor is a paradigm of classical chaotic dynamics, displaying, according to parameters, a regular, mixed, or ergodic phase space. It is also known to display accelerator modes, with a distinct ballistic behavior. In its quantum version the quantum kicked rotor (QKR) is a benchmark model for quantum simulations, intensively in the context of quantum chaos [16]. Moreover, it has been shown to display the striking phenomenon of *dynamical localization* [17,18]: At long times, the diffusive classical dynamics is inhibited by quantum effects, which have been shown mathematically to be equivalent to the Anderson localization in momentum space [19]. The first realization of the QKR using cold atoms [20] has triggered numerous experiments in the field of quantum chaos [21–24]. In particular, adding a quasiperiodic modulation of the kick amplitude allows one to map the system onto multidimensional Anderson models [25,26]. This made it possible to study two-dimensional (2D) Anderson localization [27], and to fully characterize the three-dimensional (3D) metal-insulator Anderson transition [28–32].

In this Rapid Communication, we use the cold-atom realization of the kicked rotor to (i) demonstrate that directed motion can be generated if the system's parity invariance is broken, (ii) characterize the classical anomalous diffusion of the chaotic sea, and (iii) show that the subtle quantum interferences at the origin of dynamical localization have the striking effect of counteracting this directed classical transport. At long times, the transport asymmetry associated with the ratchet dynamics disappears and the system undergoes dynamical localization, associated with a symmetrical wave function with a characteristic universal shape.

The kicked rotor is known to support so-called "accelerator" modes [33]. However, in the standard KR Hamiltonian displaying both time-reversal and parity symmetry, if some initial condition (x_0, p_0) leads to classical motion in one direction, say, $+x$, parity symmetry implies that a "conjugated" initial condition $(-x_0, -p_0)$ will lead to an equivalent motion in the $-x$ direction. Here, we use a modified Hamiltonian [34] that allows us to easily break parity symmetry,

$$\hat{H}(t) = \frac{\hat{p}^2}{2} + K \sum_n \cos(\hat{x} + a_n)\delta(t - n), \tag{1}$$

where we use dimensionless units such that the position and momentum operators obey the canonical commutation relation $[\hat{x}, \hat{p}] = i\hbar$, where $\hbar$ is an effective Planck constant that can be changed in the experiment (see below). For $a_n = 0$, $\forall n$, we retrieve the usual QKR Hamiltonian [17]. One can show that the following periodic phase-shift sequence $a_n = \varphi_{n\,[\mathrm{mod.}\,3]}$, with $\{\varphi_1, \varphi_2, \varphi_3\} = \{0, 2\pi/3, 0\}$ produces a breaking of the

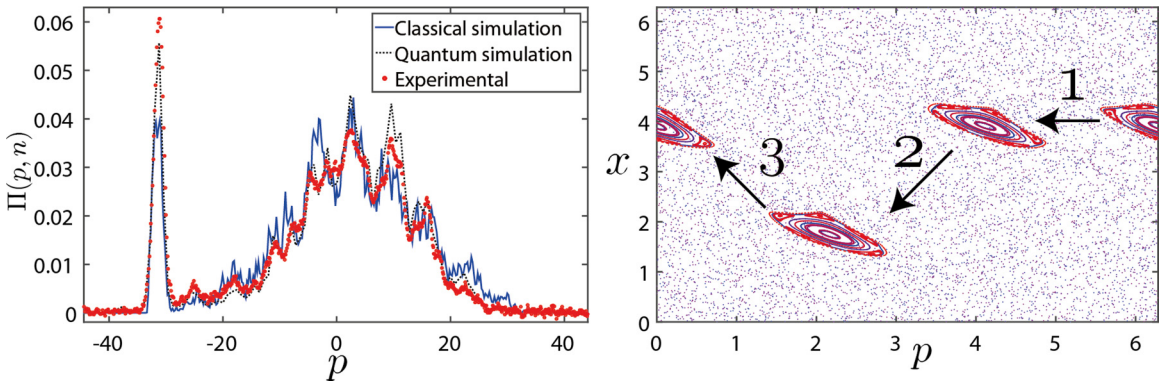

FIG. 1. Left panel: Experimental, classical (blue solid line), and quantum (red circles) momentum distributions after 15 kicks ($\bar{k} = 0.8$). Experimentally, the population of the peak at the left of the plot is 14.5%. The quantum simulation is shown as the black dashed line. Right panel: Superposition of three successive classical phase-space structures generated by the Hamiltonian (1), each corresponding to 1/3 of the full period of the system. There is thus only *one* island, whose position is displayed at each 1/3 of the period. Because the classical standard map is periodic in both x and p, it is possible to fold the phase space in the $[0,2\pi[\times[0,2\pi[$ square. In the unfolded phase space, the island is moving continuously to the left.

parity symmetry [35]. In the following, we will focus on relatively small values of $\bar{k}$, in the range 0.8–1.3, allowing us to study both the (semi)classical dynamics and dynamical localization. A similar Hamiltonian displaying an interplay between a quantum resonance, observed for $\bar{k} = 2\pi$, and accelerator modes has been studied experimentally [24,36,37]. In our case, in contrast, the ratchet effect is purely classical, and is therefore independent of the value of $\bar{k}$.

Our experiment is performed with a cold ($T \simeq 2.4\ \mu$K) cloud of cesium atoms kicked by a periodically pulsed, far-detuned standing wave ($\Delta = -13$ GHz with respect to the $D2$ line at $\sim$852 nm). The beam waist is $\sim$800 μK for a 330-m one-beam power. The standing wave is built by the overlap of two independent, arbitrarily phase-modulated, laser beams. This feature allows us to dynamically shift the potential position, and thus to synthesize Hamiltonian (1). Time is measured in units of the standing-wave pulse period T_1, space in units of $(2k_L)^{-1}$ with $k_L = 2\pi/\lambda_L$ the laser wave vector, and momentum in units of $M/2k_LT_1$ so that $\bar{k} = 4\hbar k_L^2 T_1/M$ (with M the atomic mass). At the maximum velocity reached by the atoms $v_{\max} = 0.55$ m/s, the atoms move during the pulse duration $\tau = 200$ ns of a distance $v_{\max}\tau = 110$ nm, small compared to the characteristic scale of the potential $\lambda_L/2 = 426$ nm; for most atoms one can thus consider our kicks as Dirac delta functions. For $K \propto I/|\Delta| = 3.1$ the lattice depth is about $200E_r$, where $E_r = \hbar^2 k_L^2/2M$ is the recoil energy. For these experimental parameters the decoherence time is approximately 300 kicks. The main source of decoherence are the phase fluctuations of the laser beams forming the standing wave.

The quantum dynamics of the gas can also be simulated using a Monte Carlo method: We choose a random initial momentum p_0 according to the distribution

$$|\psi_0(p)|^2 = \frac{1}{(2\pi\sigma^2)^{1/2}} e^{-\frac{p^2}{2\sigma^2}}, \tag{2}$$

which mimics the initial distribution of the atoms, where $\sigma = 1.65\bar{k}$ is the width of the thermal distribution of the atomic cloud (corresponding to $T = 2.4\ \mu$K in the experiment). The plane wave p_0 is a Bloch wave for the spatially periodic Hamiltonian (1), with Bloch vector $\beta = \mathrm{frac}(p_0/\bar{k})$, which makes it possible to propagate it using the discrete basis set composed of eigenstates of the momentum operator $|(m+\beta)\bar{k}\rangle$ with m an integer. The final momentum density is obtained by averaging the individual momentum densities over 10^4 random initial momenta. Because $\sigma \gtrsim \bar{k}$, the resulting β distribution is almost uniform.

We first analyze the short-time dynamics for a relatively small $\bar{k} = 0.8$ (corresponding to $T_1 = 7.67\ \mu$s). The left panel of Fig. 1 compares the experimentally measured momentum distribution $\Pi(p,n)$ after $n = 15$ kicks to both the classical and the quantum simulation of the dynamics. The classical result matches very well with the experiments, and demonstrates that the short-time dynamics is effectively classical. The most striking feature of the momentum distribution is the sharp peak at $p = -31.2 \simeq 15 \times (-2\pi/3)$, which will be shown to transport ballistically (in momentum) toward the left (negative p), $p_{\mathrm{peak}}(n) = -2\pi n/3$. The right panel in Fig. 1 shows the classical phase portrait obtained by evolving with the classical version of Hamiltonian (1) 2×10^5 initial conditions (x_0, p_0), with x_0 uniformly sampled and p_0 sampled according to Eq. (2). This provides a clear interpretation of the accelerator mode mechanism, corresponding to the transport of a regular island across the classical phase space. The island's center obeys the recursion condition $(x_{n+3}, p_{n+3}) = (x_n, p_n - 2\pi)$; as the maximum momentum transferred by one kick is K, changing $|p|$ by 2π each three kicks requires $K \geqslant 2\pi/3$ for the accelerator mode to exist [38]. The value $K \simeq 3.1$ we use here allows for the largest possible island.

Figure 2 (left) shows a false-color plot of the experimentally measured momentum distribution $\Pi(p,n)$ as a function of both p and n. One clearly observes the ballistic peak going to the left (at a velocity of $-2\pi/3$ per kick), and an anomalous-diffusive front propagating to the right. Indeed, it has been shown that the presence of accelerator modes is associated with an anomalous diffusion $\langle p_n^2 \rangle \propto n^\zeta$, with a nonuniversal exponent $\zeta \in [1,2]$ [10,39,40]. The momentum distribution is thus strongly asymmetric due to these very different behaviors at the right and the left wings. Furthermore, the population of the peak is seen to decrease with time.

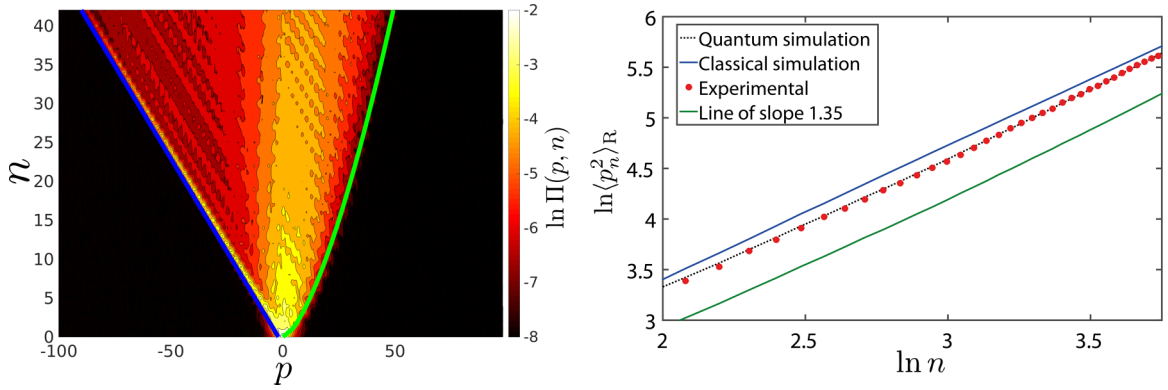

FIG. 2. Left panel: False-color plot of the experimental momentum distributions as a function of momentum p and of the number of kicks n ($\bar{k} = 0.8$). The blue line on the left shows the motion of the peak $p_{\rm peak}(n) = -2\pi n/3$, while the green line on the right shows the propagation of the anomalous-diffusion front $p_{\rm an}(n) \propto n^{\zeta/2}$. Right panel: Determination of the anomalous-diffusion exponent from the logarithmic plot of the kinetic energy of the $p > 0$ part of the system, $\langle p_n^2 \rangle_R$, as a function of the number of kicks n ($\bar{k} = 0.8$). The results of the quantum and classical simulations, as well as the experimental data, are well fitted by a power law $\langle p_n^2 \rangle_R \propto n^{\zeta}$ with $\zeta = 1.35 \pm 0.05$.

In contrast to the standard QKR, for which accelerator modes always appear in counterpropagating pairs, the fact that our setup breaks the parity symmetry allows for *directed* motion. Since an unbiased classical map, such as the one studied here, cannot display a net current when averaged over phase space [8,9], the dynamics of the chaotic sea must compensate the motion of the ballistic peak [41].

Owing to the very good resolution of our experiment, we were able to make precise measurements of the kinetic energy of the system. We can extract the kinetic energy contribution of positive momenta ($p > 0$) $\langle p_n^2 \rangle_R = \int_{p>0} p^2 \Pi(p,n) dp$, corresponding to the anomalously diffusive chaotic sea, and could thus determine by a fit the anomalous-diffusion exponent $\zeta \simeq 1.35 \pm 0.05$, which is in good agreement with both our classical and quantum simulations [see Fig. 2 (right)]. This is experimental evidence of the anomalous-diffusion behavior of the chaotic sea. Anomalous diffusion is usually interpreted in terms of chaotic trajectories which spend a long time close to the accelerated islands, thus performing Lévy flights in the *same* direction as the island [42]. Here, however, while the accelerated island propagates to the left, anomalous diffusion goes in the *opposite* direction. Thus, the precise mechanism responsible for this anomalous diffusion remains an interesting open question.

For generic values of K and $\bar{k}$, the long-time dynamics of the QKR is governed by subtle quantum interferences which lead to dynamical localization: Asymptotically, momentum distributions are exponentially localized. As the Hamiltonian of our system is time periodic (period 3) and one dimensional, one generically expects the Floquet states to be exponentially (Anderson) localized and the temporal dynamics of an initially localized wave packet to display the standard dynamical localization at long times, possibly with a very large localization length [43]. In order to observe the localization experimentally before decoherence effects become important, we have slightly increased the value of $\bar{k} \simeq 1.3$ (corresponding to $T_1 = 12.46\ \mu$s), thus reducing the localization time. The corresponding momentum distribution, for three different times, are shown in Fig. 3 (left). Note that the population in the ballistic peak decreases faster for this value of $\bar{k}$ due to the increase of quantum tunneling out of the classical island.

We observe that the distribution gradually resymmetrizes as it localizes. Quite surprisingly, the ballistic side localizes first. The anomalous-diffusion front, which propagates more slowly, localizes later, but with the same localization length. To confirm this re-symmetrization, we have performed a numerical simulation for the experimental parameters for times larger than the localization time and we observed that the

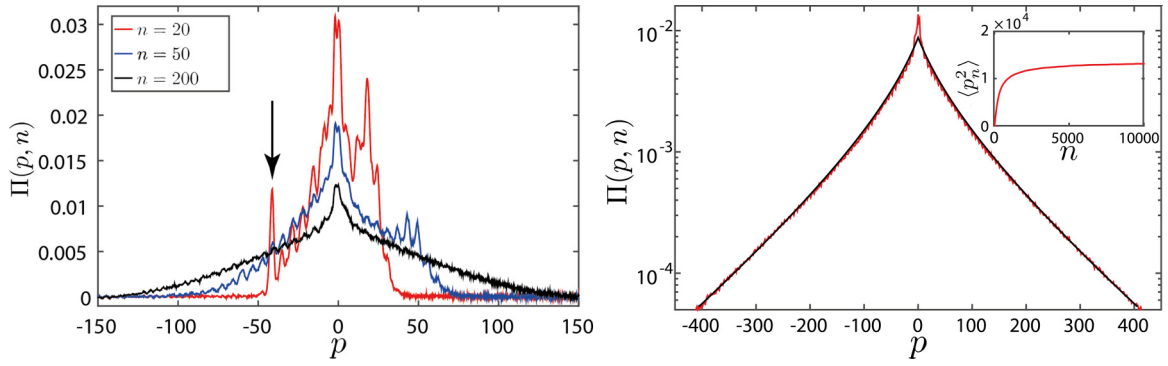

FIG. 3. Left panel: Experimental momentum distributions for $\bar{k} = 1.3$ at three different times. The arrow shows the position of the ballistic peak at $n = 20$. At $n = 200$, we observe a symmetric momentum distribution, displaying no prominent feature. Right panel: Simulated momentum distribution after $n = 10^4$ kicks (red line). The black line is the distribution (3), fitted with a localization length $\xi \simeq 35$. Inset: $\langle p_n^2 \rangle$ as a function of the number of kicks n. The numerical simulation is averaged over 5×10^4 values of the quasimomentum β.

momentum distribution at 10^4 kicks is perfectly symmetric [see Fig. 3 (right)]. The inset shows that the kinetic energy saturates due to quantum interferences, proving dynamical localization. While this resymmetrization can be surprising in the context of the QKR with directed transport, it is in fact easily understood in the context of Anderson localization: An initially well-defined wave packet (in momentum) will localize and display a universal symmetric shape, called the Gogolin distribution [44],

$$\Pi_{\mathrm{loc}}(p) = \int_0^\infty \frac{\pi^2 \eta \sinh(\pi\eta) e^{-\frac{1+\eta^2}{4\xi}|p|}}{16\xi} \left(\frac{1+\eta^2}{1+\cosh(\pi\eta)}\right)^2 d\eta. \tag{3}$$

Only the localization length ξ depends on the microscopic details, which translates here in a broad extension of the wave packet owing to the ballistic mode [45,46]. Figure 3 (right) also shows this universal distribution, which indeed describes the localized regime very well. The slight discrepancy near $p = 0$ can be understood in terms of an enhanced return to the origin effects [47] as well as the initial broadening of the wave function.

In conclusion, we have shown that the careful crafting of our experimental setup allows us to break the parity symmetry and observe a classical Hamiltonian ratchet effect accompanied by an anomalous diffusion in the short-time dynamics. At longer times, dynamical localization leads to a striking resymmetrization of the momentum distribution. It would be interesting to better characterize the mechanism leading to an anomalous diffusion in the direction opposite to the acceleration mode. Also, the quantum leaking from the classical island into the chaotic sea is important in the context of chaos-assisted tunneling [48]. This illustrates the exciting perspectives accessible when the deep classical regime ($\hbar \ll 1$) is attained experimentally. These challenging and interesting questions are left for future work.

The authors thank G. Lemarié and N. Cherroret for fruitful discussions. This work is supported by Agence Nationale de la Recherche (Grant K-BEC No. ANR-13-BS04-0001-01), the Labex CEMPI (Grant No. ANR-11-LABX-0007-01), and the Ministry of Higher Education and Research, Hauts de France Council and European Regional Development Fund (ERDF) through the Contrat de Projets Etat-Region (CPER Photonics for Society, P4S).

[1] M. Shapiro and P. Brumer, *Quantum Control of Molecular Processes* (Wiley-VCH, Weinheim, 2012).
[2] O. Morsch and M. Oberthaler, Dynamics of Bose-Einstein condensates in optical lattices, Rev. Mod. Phys. **78**, 179 (2006).
[3] A. A. Abrikosov, *Fundamentals of the Theory of Metals* (Dover, New York, 1972).
[4] F. G. Bass and A. Bulgakov, *Kinetic and Electrodynamic Phenomena in Classical and Quantum Semiconductor Superlattices* (Nova Science, New York, 1997).
[5] S. Weiss, D. Koelle, J. Müller, R. Gross, and K. Barthel, Ratchet effect in dc SQUIDs, Europhys. Lett. **51**, 499 (2000).
[6] S. Flach, O. Yevtushenko, and Y. Zolotaryuk, Directed Current Due to Broken Time-Space Symmetry, Phys. Rev. Lett. **84**, 2358 (2000).
[7] P. Reimann, Brownian motors: Noisy transport far from equilibrium, Phys. Rep. **361**, 57 (2002).
[8] T. Dittrich, R. Ketzmerick, M. Otto, and H. Schanz, Classical and quantum transport in deterministic Hamiltonian ratchets, Ann. Phys. **9**, 755 (2000).
[9] H. Schanz, M.-F. Otto, R. Ketzmerick, and T. Dittrich, Classical and Quantum Hamiltonian Ratchets, Phys. Rev. Lett. **87**, 070601 (2001).
[10] J. Gong and P. Brumer, Directed anomalous diffusion without a biased field: A ratchet accelerator, Phys. Rev. E **70**, 016202 (2004).
[11] P. Jung, J. G. Kissner, and P. Hänggi, Regular and Chaotic Transport in Asymmetric Periodic Potentials: Inertia Ratchets, Phys. Rev. Lett. **76**, 3436 (1996).
[12] J. L. Mateos, Chaotic Transport and Current Reversal in Deterministic Ratchets, Phys. Rev. Lett. **84**, 258 (2000).
[13] M. Porto, M. Urbakh, and J. Klafter, Molecular Motor that Never Steps Backwards, Phys. Rev. Lett. **85**, 491 (2000).
[14] R. Gommers, S. Bergamini, and F. Renzoni, Dissipation-Induced Symmetry Breaking in a Driven Optical Lattice, Phys. Rev. Lett. **95**, 073003 (2005).
[15] R. Gommers, S. Denisov, and F. Renzoni, Quasiperiodically Driven Ratchets for Cold Atoms, Phys. Rev. Lett. **96**, 240604 (2006).
[16] F. M. Izrailev, Simple models of quantum chaos: spectrum and eigenfunctions, Phys. Rep. **196**, 299 (1990).
[17] G. Casati, B. V. Chirikov, J. Ford, and F. M. Izrailev, Stochastic behavior of a quantum pendulum under periodic perturbation, in *Stochastic Behavior in Classical and Quantum Systems*, edited by G. Casati and J. Ford, Lecture Notes in Physics Vol. 93 (Springer, Berlin, 1979), pp. 334–352.
[18] F. L. Moore, J. C. Robinson, C. Bharucha, P. E. Williams, and M. G. Raizen, Observation of Dynamical Localization in Atomic Momentum Transfer: A New Testing Ground for Quantum Chaos, Phys. Rev. Lett. **73**, 2974 (1994).
[19] S. Fishman, D. R. Grempel, and R. E. Prange, Chaos, Quantum Recurrences, and Anderson Localization, Phys. Rev. Lett. **49**, 509 (1982).
[20] F. L. Moore, J. C. Robinson, C. F. Bharucha, B. Sundaram, and M. G. Raizen, Atom Optics Realization of the Quantum δ-Kicked Rotor, Phys. Rev. Lett. **75**, 4598 (1995).
[21] M. K. Oberthaler, R. M. Godun, M. B. d'Arcy, G. S. Summy, and K. Burnett, Observation of Quantum Accelerated Modes, Phys. Rev. Lett. **83**, 4447 (1999).
[22] P. H. Jones, M. Goonasekera, D. R. Meacher, T. Jonckheere, and T. S. Monteiro, Directed Motion for Delta-Kicked Atoms with Broken Symmetries: Comparison between Theory and Experiment, Phys. Rev. Lett. **98**, 073002 (2007).
[23] A. Kenfack, J. Gong, and A. K. Pattanayak, Controlling the Ratchet Effect for Cold Atoms, Phys. Rev. Lett. **100**, 044104 (2008).
[24] D. H. White, S. K. Ruddell, and M. D. Hoogerland, Experimental realization of a quantum ratchet through phase modulation, Phys. Rev. A **88**, 063603 (2013).
[25] D. L. Shepelyansky, Localization of diffusive excitation in multi-level systems, Physica D **28**, 103 (1987).

[26] G. Casati, I. Guarneri, and D. L. Shepelyansky, Anderson Transition in a One-Dimensional System with Three Incommensurate Frequencies, Phys. Rev. Lett. **62**, 345 (1989).

[27] I. Manai, J.-F. Clément, R. Chicireanu, C. Hainaut, J. C. Garreau, P. Szriftgiser, and D. Delande, Experimental Observation of Two-Dimensional Anderson Localization with the Atomic Kicked Rotor, Phys. Rev. Lett. **115**, 240603 (2015).

[28] J. Chabé, G. Lemarié, B. Grémaud, D. Delande, P. Szriftgiser, and J. C. Garreau, Experimental Observation of the Anderson Metal-Insulator Transition with Atomic Matter Waves, Phys. Rev. Lett. **101**, 255702 (2008).

[29] G. Lemarié, H. Lignier, D. Delande, P. Szriftgiser, and J. C. Garreau, Critical State of the Anderson Transition: Between a Metal and an Insulator, Phys. Rev. Lett. **105**, 090601 (2010).

[30] M. Lopez, J.-F. Clément, P. Szriftgiser, J. C. Garreau, and D. Delande, Experimental Test of Universality of the Anderson Transition, Phys. Rev. Lett. **108**, 095701 (2012).

[31] M. Lopez, J.-F. Clément, G. Lemarié, D. Delande, P. Szriftgiser, and J. C. Garreau, Phase diagram of the anisotropic Anderson transition with the atomic kicked rotor: Theory and experiment, New J. Phys. **15**, 065013 (2013).

[32] G. Lemarié, J. Chabé, P. Szriftgiser, J. C. Garreau, B. Grémaud, and D. Delande, Observation of the Anderson metal-insulator transition with atomic matter waves: Theory and experiment, Phys. Rev. A **80**, 043626 (2009).

[33] A. J. Lichtenberg and M. A. Lieberman, *Regular and Chaotic Dynamics* (Springer, Berlin, 1982).

[34] C. Tian, A. Kamenev, and A. Larkin, Ehrenfest time in the weak dynamical localization, Phys. Rev. B **72**, 045108 (2005).

[35] C. Hainaut, I. Manai, J.-F. Clément, J. C. Garreau, P. Szriftgiser, G. Lemarié, N. Cherroret, D. Delande, and R. Chicireanu, Controlling symmetry and localization with an artificial gauge field in a disordered quantum system, Nat. Commun. **9**, 1382 (2018).

[36] M. Sadgrove, T. Schell, K. Nakagawa, and S. Wimberger, Engineering quantum correlations to enhance transport in cold atoms, Phys. Rev. A **87**, 013631 (2013).

[37] S. Fishman, I. Guarneri, and L. Rebuzzini, A theory for quantum accelerator modes in atom optics, J. Stat. Phys. **110**, 911 (2003).

[38] Y. H. Ichikawa, T. Kamimura, and T. Hatori, Stochastic diffusion in the standard map, Physica D **29**, 247 (1987).

[39] R. Ishizaki, T. Horita, T. Kobayashi, and H. Mori, Anomalous diffusion due to accelerator modes in the standard map, Prog. Theor. Phys. **85**, 1013 (1991).

[40] T. Manos and M. Robnik, Survey on the role of accelerator modes for anomalous diffusion: The case of the standard map, Phys. Rev. E **89**, 022905 (2014).

[41] We have checked the vanishing of current explicitly in numerical simulations of the classical and quantum dynamics, and it is well verified in the experiment. The finite duration of the kicks can affect the experimental momentum distribution at large momenta, but does not change qualitatively our results. This has also been checked extensively by comparison to numerical simulations.

[42] S. Benkadda, S. Kassibrakis, R. B. White, and G. M. Zaslavsky, Self-similarity and transport in the standard map, Phys. Rev. E **55**, 4909 (1997).

[43] D. L. Shepelyansky, Some statistical properties of simple classically stochastic quantum systems, Physica D **8**, 208 (1983).

[44] K. Efetov, *Supersymmetry in Disorder and Chaos* (Cambridge University Press, Cambridge, U.K., 1997).

[45] R. Artuso and L. Rebuzzini, Effects of a nonlinear perturbation on dynamical tunneling in cold atoms, Phys. Rev. E **68**, 036221 (2003).

[46] A. Iomin, S. Fishman, and G. M. Zaslavsky, Quantum localization for a kicked rotor with accelerator mode islands, Phys. Rev. E **65**, 036215 (2002).

[47] C. Hainaut, I. Manai, R. Chicireanu, J.-F. Clément, S. Zemmouri, J. C. Garreau, P. Szriftgiser, G. Lemarié, N. Cherroret, and D. Delande, Return to the Origin as a Probe of Atomic Phase Coherence, Phys. Rev. Lett. **118**, 184101 (2017).

[48] E. V. H. Doggen, B. Georgeot, and G. Lemarié, Chaos-assisted tunneling in the presence of Anderson localization, Phys. Rev. E **96**, 040201 (2017).